EBioMedicine 56 (2020) 102800

Contents lists available at ScienceDirect

EBioMedicine

journal homepage: www.elsevier.com/locate/ebiom

Research paper

Organoid modelling identifies that DACH1 functions as a tumour promoter in colorectal cancer by modulating BMP signalling

Xiang Hu[a,b,1], Long Zhang[a,b,d,1], Yaqi Li[a,b,1], Xiaoji Ma[a,b], Weixing Dai[a,b], Xiaoxue Gao[c], Xinxin Rao[c], Guoxiang Fu[c], Renjie Wang[a,b], Mengxue Pan[c], Qiang Guo[c], Xiaoya Xu[c], Yi Zhou[c], Jianjun Gao[c], Zhen Zhang[b,e], Sanjun Cai[a,b,d,***], Junjie Peng[a,b,**], Guoqiang Hua[c,*]

[a] Department of Colorectal Surgery, Fudan University Shanghai Cancer Center, Fudan University, Shanghai 200032, China
[b] Department of Oncology, Shanghai Medical College, Fudan University, Shanghai 200032, China
[c] Institute of Radiation Medicine, and Cancer institute, Fudan University Shanghai Cancer Center, Fudan University, Shanghai 200032, China
[d] Cancer institute, Fudan University Shanghai Cancer Center, Fudan University, Shanghai 200032, China
[e] Department of Radiation Oncology, Fudan University Shanghai Cancer Center, Fudan University, Shanghai 200032, China

ARTICLE INFO

Article History:
Received 29 September 2019
Revised 28 April 2020
Accepted 29 April 2020
Available online xxx

Keywords:
DACH1
Organoid
Stem cells
BMP signalling pathway
Colorectal cancer

ABSTRACT

Background: Dachshund homologue 1 (DACH1) is highly expressed in LGR5+ intestinal stem cells and colorectal tumours. However, the roles of DACH1 in intestinal cell stemness and colorectal tumorigenesis remain largely undefined.

Methods: We used immunohistochemistry, western blotting and quantitative real-time PCR to analyse DACH1 expression in colorectal cancer (CRC) samples. CRISPR/Cas9 gene editing and lentiviral vector-mediated overexpression and shRNA-mediated knockdown of DACH1 were utilized to modulate DACH1 expression in cell lines and organoids. An intestinal organoid-based functional model was analysed, and cancer cell colony formation, sphere formation assays and murine xenotransplants were performed to reveal the role of DACH1 in CRC cell proliferation, stemness and tumorigenesis. Immunofluorescence, co-immunoprecipitation, RNA interference and microarray data analyses were conducted to demonstrate the association between DACH1 and the bone morphogenetic protein (BMP) signalling pathway.

Findings: DACH1 is specifically expressed in discrete crypt base cells, and increased DACH1 expression was found in all stages of CRC. Moreover, the high expression of DACH1 independently predicted poor prognosis. In colon cancer cells, shRNA-mediated suppression of DACH1 inhibited cell growth in vitro and in vivo. By studying the intestinal organoid-based functional model, we found that depletion of DACH1 reduced the organoid formation efficiency and tumour organoid size. DACH1 overexpression stimulated both colonsphere formation and tumour organoid formation in the context of dysregulated BMP signalling. Mechanistic characterizations indicated that overexpression of DACH1 affects a subset of stem cell signature genes implicated in stem cell proliferation and maintenance through the suppression of BMP signalling via SMAD4.

Interpretation: Together, our study highlights DACH1 as an integral regulator of BMP signalling during intestinal tumorigenesis, and DACH1 could be a potential prognostic marker and therapeutic target for colorectal cancer patients.

1. Introduction

Intestinal stem cells (ISCs) are responsible for maintaining tissue homoeostasis and are vital for tumorigenesis. ISCs are characterized by expression of the Wnt target gene *Lgr5* [1]. LGR5+ cells are actively proliferating stem cells that mediate daily renewal of the intestinal epithelium [2,3]. The fast renewal kinetics of the intestinal epithelium result in a high risk of aberrant hyperproliferation and even tumorigenesis; therefore, LGR5+ crypt base cells

* Correspondence to: Guoqiang Hua, Institute of Radiation Medicine, Fudan University, No. 2094, Xietu Road, Xuhui District, Shanghai, 200032, China
** Correspondence to: Junjie Peng, Department of Colorectal Surgery, Fudan University Shanghai Cancer Center, Director's Office, 11th floor, building 3, No. 270, Dong'an Road, Xuhui District, Shanghai, 200032, China
*** Correspondence to: Sanjun Cai, Department of Colorectal Surgery, Fudan University Shanghai Cancer Center, Director's Office, 11th floor, building 3, No. 270, Dong'an Road, Xuhui District, Shanghai, 200032, China
E-mail addresses: caisanjun_sh@163.com (S. Cai), pengjj67@hotmail.com (J. Peng), guoqianghua@fudan.edu.cn (G. Hua).
[1] These authors contributed equally to this work.

https://doi.org/10.1016/j.ebiom.2020.102800

Research in context

Evidence before this study

The tumorigenesis of colorectal cancer (CRC) is hitherto a puzzle undone. As a protein highly expressed in LGR5+ intestinal stem cells, DACH1 has been reported to play versatile roles in different cancers. However, the role of DACH1 in colorectal cancer remains controversial. Some in vitro studies suggested DACH1 as a suppressor of CRC growth and metastasis, while transcriptome analysis and IHC staining for DACH1 in normal mucosa, colorectal adenomas and colorectal carcinomas implicated DACH1 as a potential promoter of CRC tumorigenesis. However, whether and how DACH1 promotes CRC tumorigenesis remain unknown.

Added value of this study

In our study, we found that in the intestine, DACH1 is located in discrete crypt base cells. Using organoids derived from normal mucosa, colorectal adenomas and colorectal carcinomas as a model, we revealed that high expression of DACH1 is found throughout all stages of CRC and predicts poor prognosis in CRC patients. Suppression of DACH1 inhibited colon cancer cell growth in vitro and in vivo by modulating cancer cell stemness. DACH1 plays essential roles in the formation and growth of intestinal organoids. Furthermore, we found that DACH1 colocalizes and interacts with SMAD4 to compensate for the inhibition of the bone morphogenetic protein (BMP) signalling pathway by Noggin. We demonstrated that DACH1 promotes CRC tumorigenesis by modulating the BMP signalling pathway to enhance cancer cell stemness.

Implications of all the available evidence

DACH1 might be an indicator for intestinal stem cells. DACH1 is highly expressed in CRC compared with normal mucosa and promotes tumorigenesis by modulating the BMP pathway to enhance cancer cell stemness, leading to poor prognosis of CRC patients. Thus, DACH1 might be a target for CRC treatment that could be utilized for future translational medicine.

are a potential origin of intestinal tumours (colorectal adenoma and colorectal cancer (CRC)) [4]. Although Ascl2, Msi1 and Prom1 were identified as potential modulators of ISCs in mice, they lack specificity and cannot be extrapolated to humans. In-depth assessment of LGR5+ stem cells is hindered by the lack of feasible antibodies, so LGR5 has only been studied using in situ hybridization. Therefore, limited progress has been made in understanding ISC modulation in humans.

DACH1 (dachshund homologue 1) is upregulated in LGR5+ ISCs with stemness maintenance [5]. Moreover, DACH1 is expressed in a wide range of normal and cancer tissues [6–9]. However, DACH1 function varies in different tumour types and contexts; DACH1 can behave as an oncogene [8] or anti-oncogene [9]. In colorectal cancer, the role of DACH1 remains controversial [10–13]. Some studies reported DACH1 as a suppressor of proliferation and metastasis in colorectal cancer in vitro [10–12], while DACH1 was also reported to be elevated markedly in all colorectal adenomas and in most colorectal carcinomas at both the mRNA and protein levels; however, the roles of DACH1 in colorectal tumorigenesis remain unknown [13].

Here, we postulated that DACH1 serves as a putative indicator for intestinal stem cells, represents a novel mechanism underlying the modulation of ISC expansion to maintain proper intestinal homoeostasis and plays a vital role in intestinal tumorigenesis.

2. Materials and methods

2.1. Ethics statement

Written informed consent was obtained from all patients at enrolment. The research protocol was reviewed and approved by the ethics committee of FUSCC. Animal studies were approved by the Animal Ethics Committee at Shanghai Medical School, Fudan University.

2.2. Intestinal crypts, adenomas and CRC-derived organoids' culture

Organoids derived from human colon crypt, adenoma and colorectal cancer (CRC) samples were isolated and cultured as previously described [14, 15]. Briefly, isolated fresh tissues were cut into pieces and washed three times with cold PBS supplemented with 10% penicillin/streptomycin (BasalMedia, Shanghai, China). The tissues were incubated in digestion buffer (Dulbecco's modified Eagle's medium (BasalMedia) with 1% foetal bovine serum (FBS) (Thermo Fisher Scientific, MA, USA), 10% penicillin/streptomycin, 1.5 mg/mL collagenase type II, 500 U/mL type collagenase IV, 0.1 mg/mL dispase type II and 10 μM Y-27,632 (Selleck, Shanghai, China)) for 45 min at 37 °C with vigorous vibration. After digestion, the crypt fraction and tumour pellets were washed with PBS 3 times to remove digestion enzymes and were finally collected through centrifugation at 200 g for 5 min. Then, the crypts and tumour pellets were embedded in Matrigel (Corning, NY, USA) and plated in 24-well plates. After the polymerization of the gel, organoid culture medium (Advanced DMEM/F12 (Thermo Fisher Scientific) supplemented with Noggin (Sino Biological Inc., Beijing, China), R-spondin (Sino Biological Inc.), EGF (Sino Biological Inc.), GlutaMAX (Thermo Fisher Scientific), HEPES (Thermo Fisher Scientific), N2 (Thermo Fisher Scientific), B27 (Thermo Fisher Scientific), N-acetylcysteine (Merck Sigma-Aldrich, MA, USA), Gastrin (Merck Sigma-Aldrich), Nicotinamide (Merck Sigma-Aldrich), A83-01 (Tocris Bioscience, MN, USA) and SB202190 (Merck Sigma-Aldrich)) was added. The medium was changed approximately every 3 days, and organoids were passaged approximately every 7 days according to their growth conditions.

2.3. Patient specimens, cell lines and stable organoids

For immunohistochemistry (IHC), samples of CRC patients were obtained consecutively and randomly from Fudan University Shanghai Cancer Centre (FUSCC) between 2007 and 2009. Only patients with fully characterized tumours, intact overall survival (OS) and disease-free survival (DFS) information were included. All patients' data were collected, including age, sex, race, tumour location, year of diagnosis, primary tumour size, histological grade, number of lymph nodes examined, type of radiation, marital status, preoperative multimodal treatment, details of the surgical procedure, occurrence of complications, postoperative histopathology, application of adjuvant therapy, and follow-up (date of last visit, tumour recurrence, date of tumour-related or unrelated death, overall survival and disease-free survival). For organoid culture, colorectal adenoma, CRC and adjacent normal intestinal tissues were obtained from patients diagnosed and treated at FUSCC. HCT116 (RRID:CVCL_0291) and SW620 (RRID: CVCL_0547) colon cancer cell lines were obtained from Type Culture Collection Cell Bank, Chinese Academy of Sciences, authenticated by short tandem repeat (STR) analysis and cultured in DMEM (GE China Hyclone, Beijing, China) with 10% FBS (Thermo Fisher Scientific) at 37 °C and a 5% CO_2 atmosphere in a cell incubator. Lentiviral constructs containing human DACH1 cDNA or empty vector (as a control) and shRNA targeting human DACH1 (shDACH1) or scrambled sequence (as a negative control, shNC) (all purchased from Obio Technology, Shanghai, China) were used for DACH1 overexpression and knockdown, respectively. To generate stable cell lines and stable organoids, HCT116 and SW620 colon cancer cell lines and organoids

were infected with the corresponding viruses and selected with puromycin (Solarbio, Shanghai, China). Stable cell lines and stable organoids were confirmed for DACH1 overexpression or knockdown by western blotting or quantitative real-time PCR (qRT-PCR). For organoids in which DACH1 was knocked out, three single guide-RNAs (designated sg1, sg2, and sg3) targeting the *DACH1* gene and a control gRNA targeting none (designated NT) were generated and then transfected into human CRC organoids with Cas9 expression. After selection, *DACH1* knockout was confirmed by western blotting. Small interfering RNAs (siRNA) targeting human SMAD4 and scrambled negative control (siNC) were obtained from GenePharma company (Shanghai, China) and were transfected into noted cell lines using Highgene transfection reagent (Abclonal, Wuhan, China) following the manufactures' guide.

2.4. RNA-seq and data analysis

Organoids derived from human colorectal adenomas stably overexpressing DACH1 or empty vector as a control were cultured in organoid complete medium for 5 days. Total RNA was extracted from 10^6 single cells and reversely transcribed into cDNA libraries according to the manual's instructions. The Illumina HiSeq 2000 platform was used for high-throughput sequencing with two biological replicates. Gene set enrichment analysis (GSEA) was carried out with the GSEA platform of the Broad Institute (http://www.broadinstitute.org/gsea/index.jsp). GO analysis was performed with a hypergeometric test by using differentially expressed genes against gene sets from the GO database (http://geneontology.org/) and KEGG pathway database (http://www.genome.jp/kegg/pathway.html).

2.5. Xenotransplant murine models

A total of 5×10^6 cells were suspended in 100 μL Matrigel and injected subcutaneously into the right flank of athymic nude mice (n = 5, male). Xenotransplant growth was monitored using callipers every 3 days, and animals were euthanized after approximately 4 weeks. Xenotransplants were harvested, weighed, fixed in formalin and paraffin embedded for pathological analysis. Xenotransplant volumes were calculated using the following equation: volume = $(d^2 \times D)/2$, where D is the long side and d is the short side of a xenotransplant.

2.6. Colony formation assays

For colony formation assays, 500 cells established from HCT116 or SW620 cell lines were seeded in a well of a 6-well plate and cultured for 14 days. Cell colonies were fixed with 4% paraformaldehyde/PBS (Yeasen, Shanghai, China) for 30 min and then stained with 2% crystal violet (Yeasen) for 30 min at room temperature, after which the colonies were washed with PBS 3 times and dried. Representative images were captured to quantify the colonies for colony formation efficiency calculation. The assays were repeated three times independently.

2.7. Immunohistochemistry (IHC) and immunofluorescence (IF)

Briefly, for IHC, after deparaffinizing tissue slides using xylol, the antigen retrieval procedure was carried out in sodium citrate (pH 6.0) at 100 °C for 15 min. After endogenous peroxidase activity elimination by 3% H_2O_2, sections on slices were blocked with 1% BSA/PBS (Sangon, Shanghai, China), followed by primary antibody incubation in a humidified chamber overnight at 4 °C. Primary antibodies were purchased from Cell signalling Technology (CST, MA, USA) or Proteintech Group (Wuhan, China): anti-DACH1 (Proteintech Cat. 10914-1-AP, 1:600), anti-SMAD4 (CST, Cat.#46535, 1:400), anti-CD166 (Proteintech, Cat. #21972-1-AP, 1:200), anti-OLFM4 (CST, Cat. #14369, 1:400), and anti-Sox2 (CST, Cat. #14962, 1:400). After washing with PBS, horseradish peroxidase (HRP)-conjugated anti-rabbit/mouse secondary antibodies (Gene Technology, Shanghai, China) were applied and incubated for 1 h. The sections were then developed using GTvision TM III (Gene Technology), counterstained with 10% haematoxylin (Solarbio), dehydrated and mounted with resinene (Solarbio). The staining intensity was scored as 0 (negative), 1 (weak), 2 (medium) or 3 (strong). The extent of staining was scored as 0 (<5%), 1 (5−25%), 2 (26−50%), 3 (51−75%) or 4 (>75%) according to the percentages of the positive staining areas in relation to the whole carcinoma area. We multiplied the percentage score by the staining intensity score to generate the immunoreactivity score (IRS). For IF experiments, antigen retrieval of the sections and incubation of the sections with the SMAD4 primary antibody were performed as described for the IHC protocol above. Then, the secondary antibody (Alexa Fluor 488 anti-rabbit antibody (1:200), Thermo Fisher Scientific) was applied and incubated with the sections for 1 h at room temperature. For DACH1 staining, a CoraLite594-conjugated DACH1 antibody (Proteintech, Cat. CL594-60082, 1:200) was used. Ultimately, nuclei were counterstained with DAPI for 5 min and mounted. Fluorescence images were captured with a Leica TCS-SP5 confocal system (IL, USA).

2.8. Western blotting (WB) and co-immunoprecipitation (CoIP)

For WB, briefly, primary antibodies were purchased from Cell signalling Technology, Affinity Biosciences (OH, USA), Abclonal, Proteintech, or MBL (Janpan). Anti-DACH1 antibody (Proteintech Cat. 10914-1-AP, 1:1000), anti-SMAD4 antibody (CST, Cat. #46535, 1:1000), anti-Phospho-Smad4 (Thr276)[Thr277] antibody (Affinity Biosciences, Cat. AF8316, 1:1000), anti-LGR5 antibody (Abclonal, Cat. A10545, 1:1000), anti-NICD (Cleaved-Notch 1 (Val1744) antibody, Affinity Biosciences, Cat. AF5307, 1:1000), anti-GAPDH antibody (Proteintech, Cat. 10494-1-AP, 1:5000) and anti-FLAG (Anti-DDDDK-tag) antibody (MBL, M185-3 L, 1:5000) were incubated with the membrane respectively, followed by washing for 3 times with TBST and incubation with according HRP-conjugated secondary antibodies. After washing off the unbound secondary antibodies with TBST, the bands were detected using LAS 4000 (GE, MA, USA). For CoIP, total cell lysates were incubated with anti-DACH1 or anti-SMAD4 antibody followed by incubation with protein G-Sepharose beads (Thermo Fisher Scientific). The beads were washed three times with lysis buffer. The immunoprecipitates were eluted by boiling the beads for 5 min in SDS loading buffer and subjected to WB as described above.

2.9. Quantitative real time-PCR (qRT-PCR)

Total RNA was extracted from patient-derived tissues or organoids or colon cancer cells using TRIzol reagent (Thermo Fisher Scientific) according to the manufacturer's instructions. cDNA was acquired by reverse transcription of RNA using PrimeScript™ RT Master Mix (Takara Bio Inc. Dalian, China). qRT-PCR assays were performed on a QuantStudio™ 7 Flex Real-Time PCR System (Thermo Fisher Scientific) following standard protocols using SYBR® Premix Ex Taq™ II (Tli RNase H Plus) (Takara). The housekeeping gene *GAPDH* was set as an endogenous control for every sample, and the expression of genes in different samples was calibrated to that of the corresponding normal tissues or control organoids or control cells. Data were analysed using QuantStudio Real-Time PCR Software (Thermo Fisher Scientific) and GraphPad Prism 7 (La Jolla, CA, USA).

2.10. Sphere formation assay

To examine the effects of DACH1 on cancer stem cell phenotypes, a sphere formation assay was conducted. Briefly, stable cell lines established from HCT116 cells were harvested, washed with PBS twice, and counted. Five hundred cells were plated in a well of a 96-well plate containing 200 μL serum-free medium for sphere

formation (DMEM/F12; 3:1 mixture (Thermo Fisher Scientific) containing 0.4% BSA (Sangon), 0.2 × B27 (Thermo Fisher Scientific), recombinant EGF (Sino Biological Inc.) at 10 ng/mL, and bFGF (Pepro-Tech China, Jiangsu, China) at 10 ng/mL). After 10 days, the spheres were counted, and images were taken.

2.11. Statistical analysis

In this study, data obtained from cell and organoid experiments were analysed using Student's t-test, and the results are presented as the mean±SD. For clinical data, the mRNA expression levels and the immunoreactivity scores of DACH1 were analysed using Student's t-test and presented as the mean±SD. Survival analysis was conducted using the Kaplan−Meier method, and a log-rank test was used to determine the significance of the differences. To determine the association between DACH1 expression and patient prognosis, Cox regression analysis was conducted, and the significance was determined using the log-rank test. Fisher's exact test or a two-tailed χ^2 test was used to define the relationship between the expression of DACH1 and patient characteristics. Confidence intervals (CIs) were stated at the 95% confidence level. All analyses were conducted using SPSS software (version 22.0; SPSS, Chicago, IL) and GraphPad Prism 7, and P-values < 0.05 were considered statistically significant.

2.12. Data sharing

The data of RNA seq for human colorectal adenomas organoids stably overexpressing DACH1 or empty vector as a control were deposited in Mendeley Data (https://data.mendeley.com).

2.12.1. Data set name

RNA seq data of 2 colorectal adenoma organoids overexpressing DACH1 and their controls for "Organoid modelling identifies that DACH1 functions as a tumour promoter in colorectal cancer by modulating BMP signalling" DOI: 10.17632/cw6kdksp5b.1

3. Results

3.1. DACH1 is expressed in crypt base cells of the intestine

To identify the expression pattern of DACH1, IHC and IF were performed in the small and large intestines of mice. The results demonstrated that DACH1 is localized in the nuclei of crypt base cells in the intestine (Fig. 1a-1d). In the mouse small intestine, DACH1 positive cells were located along the crypt base, which is comprised of both base columnar cells and Paneth cells (Fig. 1a). To demarcate the DACH1 positive cells in the small intestines, both DACH1 (green) and lysozyme (a marker of Paneth cells, red) were detected using IF, and the nuclei were stained with DAPI (blue). The result showed that DACH1 staining cells (green) were interspersed between the Paneth cells (red) in all of the crypts (Fig. 1c). A similar expression pattern was observed in the mouse large intestinal crypts (Fig. 1b). DACH1 expressing cells in the human colon exhibited a slender morphology and were interspersed between the goblet cells at the crypt base (Fig. 1d). These data indicate that DACH1 is expressed in the crypt base cells of the intestine.

3.2. DACH1 is overexpressed in all stages of human CRC

It has been previously reported that DACH1 is overexpressed in tumours, and its expression in crypt base cells implies a role in CRC. To validate this, qRT-PCR analysis was performed in a series of colorectal normal tissues (n = 22) and CRC tissues (n = 22). We found that the DACH1 mRNA level was significantly higher in CRC tissues than in adjacent normal tissues (Fig. 1e, $^{*}P < 0.05$, Student's t-test). The DACH1 protein level was validated by IHC in a series of normal colorectal tissues (n = 18) and stage I to IV CRC tissues. DACH1 expression was increased in all stages of CRC compared with that in normal tissue (Fig. 1f, $^{*}P < 0.05$, $^{**}P < 0.01$, $^{***}P < 0.001$, Student's t-test). Additionally, elevated DACH1 expression was directly observed at the invasive front of the tumour lesion located at the boundary between the normal area and the tumour area (Fig. 1g). Hence, these data indicate that DACH1 is overexpressed in all stages of CRC at both the mRNA level and the protein level.

3.3. High expression of DACH1 predicts a poor prognosis in crc patients

The overexpression of DACH1 in CRC compared with adjacent normal tissues implies its oncogenic role. To assess the relationship between DACH1 expression and clinical outcomes of CRC patients, patients were stratified into two groups: low expression (low, IRS ≤ 4, n = 118) and high expression (high, IRS > 4, n = 89) of DACH1. The demographic and baseline clinical data are shown in Table 1, including sex, diagnostic age, histological type, TNM stage, pathological grade, venous/perineural invasion, MSI/MMR status, and adjuvant therapy in FUSCC cohorts. Cox regression analysis was carried out to test the association between DACH1 expression and patients' prognosis. DACH1 expression, TNM stage, venous invasion, adjuvant therapy and CEA status were independent prognostic factors for CRC patients according to the univariate Cox regression model (P = 0.005, Table 2, Cox regression analysis). Consistently, multivariate analysis after adjustment also indicated that DACH1 expression, TNM stage, adjuvant therapy and CEA status were independent factors predicting the survival of CRC patients ($P < 0.05$, Cox regression analysis). Kaplan-Meier analysis demonstrated that high DACH1 expression was markedly associated with poor prognosis, with an overall survival (OS) of 58 months in the DACH1 high group compared with 76 months in the DACH1 low group (Table 2, $P < 0.001$, Cox regression analysis). Disease-free survival (DFS) also showed a pattern similar to that of OS according to the univariate Cox proportional hazards model of risk factors (Table 3, $P < 0.001$, Cox regression analysis). The multivariate Cox proportional hazards model confirmed that DACH1 was independently associated with poor DFS (P = 0.023, Cox regression analysis). Accordingly, survival analysis for DACH1 expression validated that higher DACH1 expression was significantly correlated with shorter OS (Fig. 1h, $P < 0.001$, log-rank test) and DFS (Fig. 1i, $P < 0.001$, log-rank test).

3.4. DACH1 suppression inhibits colon cancer cell growth in vitro and in vivo

Because DACH1 expression is elevated in CRC, we investigated the effect of DACH1 suppression on colon cancer cell migration and proliferation in vitro. DACH1 expression was stably knocked down in the human colon cancer cell lines SW620 and HCT116 (Fig. 2a). To assess the role of DACH1 in migration, a transwell chamber migration assay and a scratch assay were performed. Suppression of DACH1 in SW620 and HCT116 cells did not lead to significantly reduced cell migration (Supplementary data, Fig. S1). Then, we investigated the role of DACH1 in cell survival and growth using a colony formation assay. As shown in Fig. 2b and 2c, DACH1 knockdown significantly inhibited the colony formation rate in both cell lines ($^{**}P < 0.01$, $^{***}P < 0.001$, Student's t-test). Additionally, we established a murine xenograft model to verify the role of DACH1 in vivo. Suppression of DACH1 in HCT116 cells caused a significant decrease in xenograft volume and weight (Fig. 2d-2f, $^{*}P < 0.05$, Student's t-test). Given that DACH1 is expressed in crypt base cells, we further investigated the effect of DACH1 on stem cell-like phenotypes. The results of sphere formation assay showed that knocking down of DACH1 significantly reduced the number of the spheres formed by HCT116 cells (Fig. 2g and 2h, $^{*}P < 0.01$, Student's t-test). Additionally, we detected stem cell markers in xenograft sections

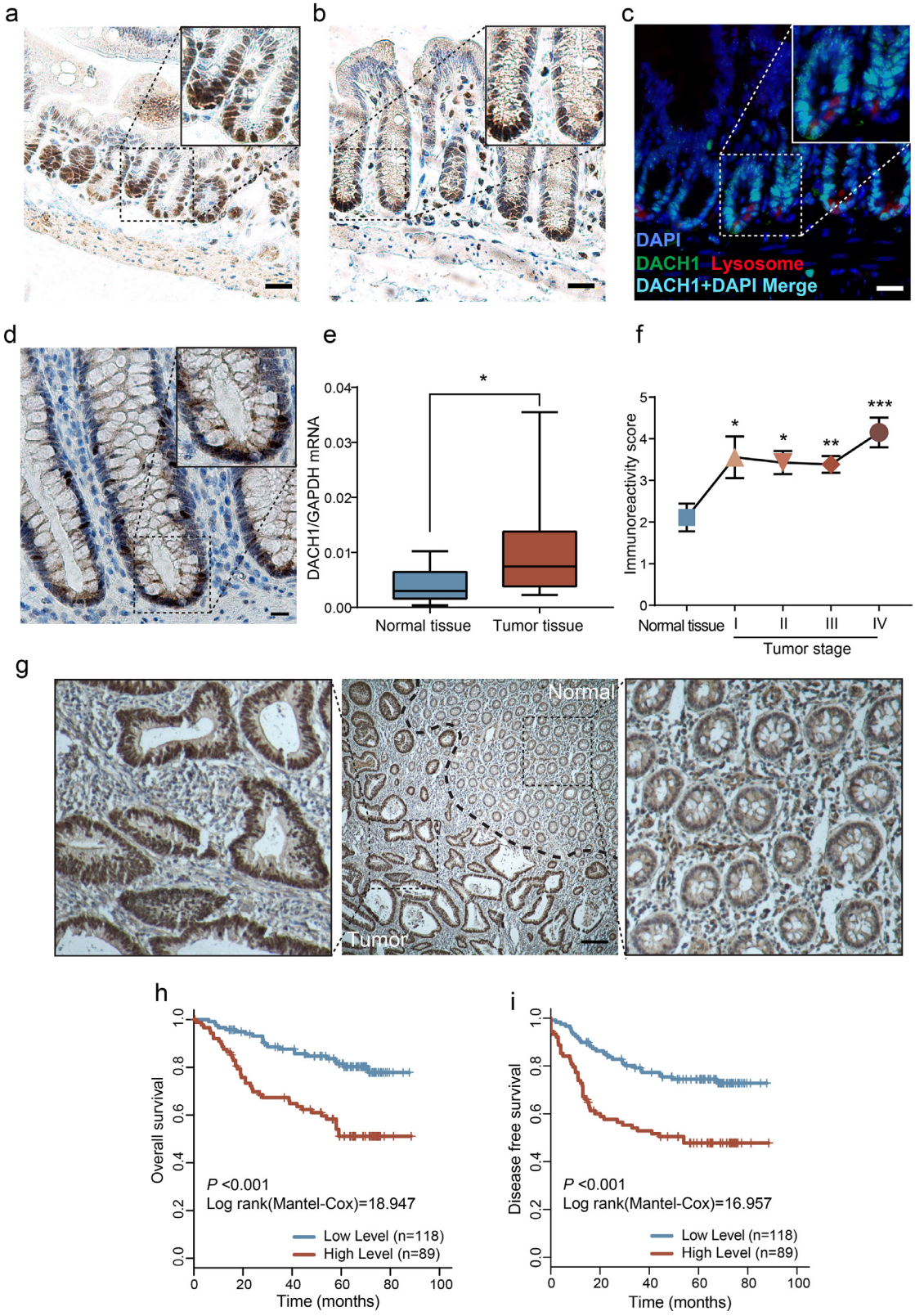

Fig. 1. DACH1 marks crypt base cells in intestines and predicts poor outcomes in colorectal cancer patients. DACH1 expression in the mouse small intestine (a) and large intestine (b); scale bars=20 μm. In the mouse small intestine, DACH1 is expressed in crypt base cells interspersed between Paneth cells. Lysozymes (a marker of Paneth cells) were stained red, and DACH1 was stained green, which merged into cyan with DAPI (blue); scale bar=20 μm (c). DACH1 is also expressed in the human large intestine; scale bar=20 μm (d). DACH1 mRNA is overexpressed in colorectal cancer tissues compared to adjacent normal tissues, as detected by qRT-PCR (e), and IHC revealed that the expression of DACH1 increased in all stages of CRC when compared with the normal tissue (f) ($^{*}P < 0.05$, $^{**}P < 0.01$, $^{***}P < 0.001$, Student's t-test; error bars: mean±SD). Elevated DACH1 expression at the invasive front of the tumour lesion; scale bar=100 μm (g). Kaplan-Meier survival analyses based on DACH1 expression for overall survival (h, $P < 0.001$, log-rank test, between high level and low level of DACH1) and disease-free survival (i, $P < 0.001$, log-rank test, between high level and low level of DACH1).

Table 1
Baseline characteristics in patients with high and low expression of DACH1.

Variables, N (%)	DACH1 expression		P value
	Low (n = 118)	High (n = 89)	
Gender			
Male	51(43.2)	30(33.7)	0.165
Female	67(56.8)	59(66.3)	
Age, years	57.5 ± 10	58.4 ± 10	0.527
TNM stage			0.001
I	11(9.3)	5(5.6)	
II	44(37.3)	20(22.5)	
III	54(45.8)	40(44.9)	
IV	9(7.6)	24(27.0)	
T stage			0.25
T2	19(16.1)	9(10.1)	
T3	24(20.3)	14(15.7)	
T4	75(63.6)	66(74.2)	
N stage			0.054
N0	61(51.7)	32(36.0)	
N1	33(28.0)	26(29.2)	
N2	24(20.3)	30(33.7)	
M stage			<0.001
M0	109(92.4)	65(73.0)	
M1	9(7.6)	24(27.0)	
Grade			0.03
Well/ moderate	88(74.6)	68(76.4)	
poor	19(16.1)	20(22.5)	
Histological type			0.132
Adenocarcinoma	110(93.2)	87(97.8)	
Mucinous	8(6.8)	2(2.2)	
Lymph node examined			0.34
Median	15 ± 6	14 ± 5	
Perineural invasion			0.648
Negative	100(85.5)	74(83.1)	
Positive	17(14.5)	15(16.9)	
Vascular invasion			0.13
Negative	80(67.8)	54(60.7)	
Positive	35(29.7)	35(39.3)	
Adjuvant Chemotherapy			0.004
No	23(19.5)	18(20.2)	
Yes	86(72.9)	50(56.2)	
MS status/MMR status			0.08
MSS/MMR-proficient	79(66.9)	49(55.1)	
MSI/MMR-deficient	39(33.1)	40(44.9)	
CEA (ng/mL)	38.5 ± 13.7	23.4 ± 12	0.42

MMR indicates mismatch repair; MS, microsatellite; MSS, microsatellite stability; MSI, microsatellite instability.

using IHC. As shown in Fig. 2i, xenografts derived from HCT116-shDACH1 cells showed weaker CD166, OLFM4 and SOX2 staining than control cells. Collectively, these results suggest that DACH1 is essential for colon cancer cell survival and growth in vitro and in vivo, which may result from a direct effect of DACH1 on the induction of cancer stem cells.

3.5. DACH1 is essential for CRC organoid formation

Self-renewal of CRC organoids indicates the existence of cancer stem cells, and our findings suggest that there is an association between DACH1 and cell stemness. Thus, to illustrate the role of DACH1 in maintaining cancer stem cells, we prepared organoids from resected primary human CRC tissues and knocked out DACH1 using the clustered regularly interspaced short palindromic repeats (CRISPR)-Cas9 system. Compared with the control (NT), single guide RNAs (sg1/sg2/sg3) exhibited efficient knockout of DACH1 (Fig. 3b). During the sphere growth period, the total sphere area of DACH1-knockout organoids was significantly smaller than that of NT organoids (Figs. 3a and c, $^{**}P < 0.01$, Student's t-test). The subhistogram displays the area distribution of the organoids in quartiles (Figs. 3d and e). The red and green colours represent the 25th and 75th quartiles, respectively, of the distribution with increased areas of organoids. The length of the coloured area represents the number of spheres with the corresponding size range. Organoid areas in the presence of DACH1 expression were found to be much larger than those with DACH1 depletion (Fig. 3d and 3e). At the peak cellular effect, the average sphere area in DACH1 knockout organoids was much smaller than that in control organoids (Fig. 3f and 3g, $^{*}P < 0.05$, $^{**}P < 0.01$, $^{***}P < 0.001$, Student's t-test). The sphere area in the NT group organoids at day 11 increased to approximately 5-fold of that at day 2, while that in the DACH1 knockout organoids only increased by approximately 3-fold (Fig. 3h and 3i, $^{*}P < 0.05$, $^{**}P < 0.01$, $^{***}P < 0.001$, Student's t-test). Moreover, after DACH1 knockout, the sphere forming efficiency fell from 80% to 50% (Fig. 3j and 3k, $^{***}P < 0.001$, $^{****}P < 0.0001$, Student's t-test). These data indicate that DACH1 plays an essential role in CRC organoid formation and stemness.

3.6. Elevation of DACH1 expression enhances colonoid formation

Cancer stem cells utilize mechanisms employed by normal stem cells to achieve tumour survival and development. Therefore, we used organoids derived from normal colon crypts (colonoids) to further confirm the role of DACH1 in promoting cell stemness. Colonoids were digested into single cells, which are supposed to round up into spheres within 24 h. However, the colonoid formation efficiency observable at day 6 was only 30% (Fig. 4c and 4e). In cells overexpressing DACH1 (Fig. 4a and 4b, $^{*}P < 0.05$, Student's t-test), the colonoid formation efficiency at day 6 increased to 50% (Fig. 4c and 4e,

Table 2
Univariate and multivariate analysis for overall survival.

	Univariate analysis			Multivariate analysis		
Variables	Hazard ratio	95% CI	P value	Hazard ratio	95% CI	P value
DACH1 (high)	3	1.782–5.052	<0.001	2.177	1.263–3.755	0.005
Male gender	0.7	0.411–1.193	0.19	NA		
Age >70	1.235	0.750–2.034	0.407	NA		
T stage, T4	6.55	1.595–6.925	0.009	1.712	1.014–2.890	0.044
N stage, N2	4.05	2.140–7.655	<0.001	1.326	0.934–1.883	0.115
M1 stage	9.23	5.502–5.487	<0.001	2.803	1.266–6.204	0.011
Grade, poor	1.38	0.834–2.306	0.21	0.931	0.3–2.891	0.901
Lymph node examined	0.613	0.326–1.151	0.128	NA		
Mucinous Adenocarcinoma	0.567	0.139–2.321	0.43	NA		
Perineural invasion	1.557	0.845–2.87	0.156	NA		
Vascular invasion	2.038	1.252–3.319	0.004	0.91	0.721–2.066	0.459
Adjuvant therapy	2.599	1.892–3.571	<0.001	1.78	1.205–2.634	0.004
MSI	1	0.599–1.667	0.999	NA		
CEA >10 ng/mL	1.841	1.151–2.943	0.01	1.91	1.159–3.151	0.011

MMR indicates mismatch repair; MS, microsatellite; MSS, microsatellite stability; MSI, microsatellite instability; LN, lymph nodes.

Table 3
Univariate and Multivariate analyses of prognostic factors for disease-free survival.

	Univariate Analysis			Multivariate Analysis		
Variables	Hazard ratio	95% CI	P value	Hazard ratio	95% CI	P value
DACH1 (high)	2.251	1.606–4.053	<0.001	1.76	1.079–2.874	0.023
Male gender	0.674	0.415–1.095	0.111	NA		
Age >70	1.185	0.752–1.868	0.464	NA		
T stage, T4	5.294	1.661–16.871	0.005	1.558	0.977–2.487	0.063
N stage, N2	3.735	2.098–6.649	<0.001	1.207	0.881–1.654	0.24
M1 stage	9.892	6.064–16.136	<0.001	7.249	3.968–13.241	<0.001
Grade, poor	1.233	0.779–1.953	0.371	NA		
Lymph node examined	0.635	0.349–1.155	0.137	NA		
Mucinous Adenocarcinoma	0.447	0.110–1.823	0.262	NA		
Perineural invasion	1.514	0.859–2.669	0.152	NA		
Vascular invasion	1.832	1.175–2.857	0.008	0.751	0.449–1.255	0.274
Adjuvant therapy	0.689	0.335–1.419	0.313	NA		
MSI	0.97	0.611–1.539	0.896	NA		
CEA >10 ng/mL	1.588	1.040–2.425	0.032	1.421	0.910–2.218	0.122

MMR indicates mismatch repair; MS, microsatellite; MSS, microsatellite stability; MSI, microsatellite instability; LN, lymph nodes.

$^{***}P < 0.001$, Student's t-test). Moreover, the proliferation of colonoid cells increased significantly, as shown in Fig. 4c and 4d ($^{*}P < 0.05$, $^{**}P < 0.01$, Student's t-test). These data indicate that DACH1 also enhances the stemness of normal ISCs, further confirming the role of DACH1 in stemness maintenance.

3.7. DACH1 promotes the growth of adenoma organoids

The signalling events during intestinal regeneration and tumorigenesis show notable similarities. Hence, adenomas were utilized for further studies. After 7 days, DACH1-overexpressing adenoma organoids (Fig. 4f, $^{**}P < 0.01$, Student's t-test) expanded to approximately twice the size of the controls (Fig. 4h and 4i). Additionally, as displayed in Fig. 4i, there was a significant increase in growth induced by DACH1 ($^{*}P < 0.05$, $^{**}P < 0.01$, Student's t-test). After culture for 7 days, adenoma cells that overexpressed DACH1 had an organoid-forming efficiency of 70%, yet that of the control was <50% (Fig. 4j, $^{**}P < 0.01$, Student's t-test). When analysing the distribution pattern of organoid areas, DACH1-overexpressing organoids occupied more of the lower quartile and less of the upper quartile than the control organoids (Fig. 4k-4l). Moreover, the median organoid area of DACH1-overexpressing organoids was larger (50%) than that of the control (Fig. 4m and 4n). These data indicate that the role of DACH1 in promoting stemness also applies to adenoma organoids, which were used in further investigations.

3.8. DACH1 induces the upregulation of stem cell signature genes by inhibiting the BMP signalling pathway

To reveal the mechanisms underlying the functional consequences of DACH1, we performed RNA-seq analysis using RNAs isolated from control or DACH1-overexpressing adenoma organoids. The analysis revealed that overexpression of DACH1 induced a significant upregulation of cancer stem cell marker s, such as YAP, Msi2, Sox9 and Notch1 (Fig. 5a). Gene ontology (GO) analysis highlighted that DACH1 induced the upregulation of genes that account for stem cell maintenance (Fig. 5b) and the downregulation of genes involved in cell cycle arrest (Fig. 5c). These findings prompted us to test whether DACH1 induced cell stemness through transcriptional pathways. RNA-seq analysis identified significantly enriched changes in the BMP signalling pathway induced by DACH1. Verification experiments revealed that DACH1 induced the downregulation of ATOH8, TGFβ3, MSX1, NBL1, BMP7, and FKBP4. However, DACH1 induced the upregulation of FKBP8, ID1, and MAPK3 (Figs. 5d and e, $^{*}P < 0.05$, Student's t-test). These results suggest an association between DACH1 and the BMP signalling pathway, in which SMAD proteins are master mediators [16,17]. To reveal the relationship between DACH1 and SMAD proteins, we performed IF experiments. As shown in Fig. 5f, DACH1 and SMAD4 colocalized in nuclei, providing a subcellular location in which their interaction may occur. Furthermore, we performed CoIP experiments to verify the physical interaction between DACH1 and SMAD4 in cells. The results showed that SMAD4 was detected in the immunoprecipitates of the DACH1 antibody and vice versa, verifying the physical interaction between DACH1 and SMAD4 (Figs. 5g and h). To determine the influence that DACH1 has on SMAD4, we overexpressed FLAG-tagged DACH1 in HCT116 cells (Fig. 5i). Surprisingly, western blotting analysis revealed that overexpression of DACH1 elevated the protein level of SMAD4 while decreased the level of phosphorylated SMAD4 (Thr276)[Thr277] (Fig. 5i). Although FKBP8, ID1, and MAPK3 were shown to be decreased in the results of RNA-seq (Fig. 5a), we still detected an increase of these genes in our verification experiments (Fig. 5e). The discordance of the results prompted us to further exploration. To verify the SMAD4 downstream genes that were influenced by DACH1, we knocked down SMAD4 in HCT116-shDACH1 cells (Figs. 5j and k, $^{*}P < 0.05$, $^{**}P < 0.01$, Student's t-test). Knockdown of DACH1 increased the mRNA levels of NBL1 and BMP7, but did not bring a significant change to the mRNA level of SMAD4 (Fig. 5k, $^{*}P < 0.05$, $^{**}P < 0.01$, Student's t-test). While SMAD4 decrease eliminated the increases of NBL1 and BMP7 that was induced by DACH1 knockdown (Fig. 5k, $^{*}P < 0.05$, $^{**}P < 0.01$, Student's t-test). Together, these data imply that DACH1 repressed the BMP signalling pathway by decreasing the phosphorylation of SMAD4 and inhibiting the expression of NBL1 and BMP7 through interacting with SMAD4.

3.9. DACH1 exerts its function through modulating the BMP signalling pathway, but not the EGF or WNT signalling pathways

To further confirm that DACH1 inhibits the BMP signalling pathway to promote cell stemness and, thus, organoid formation, we withdrew different factors from the organoid medium.

Noggin promotes stem cell survival in intestinal crypts by antagonizing the BMP signalling pathway [18]. After depletion of Noggin from the medium, adenoma organoid formation was significantly reduced (Fig. 5l). However, DACH1 overexpression reversed the inhibition of organoid formation induced by Noggin depletion (Fig. 5l). As DACH1 repressed the expression of NBL1 and BMP7 (Fig. 5k, $^{*}P < 0.05$, $^{**}P < 0.01$, Student's t-test), we detected whether Noggin could affect NBL1 and BMP7 in a similar way. As shown in Fig. 5m ($^{*}P < 0.05$, Student's t-test), after the addition of Noggin into the medium of HCT116 cells for 24 h and 36 h, the increased mRNA levels of NBL1 and BMP7 by DACH1 knockdown were reduced by the

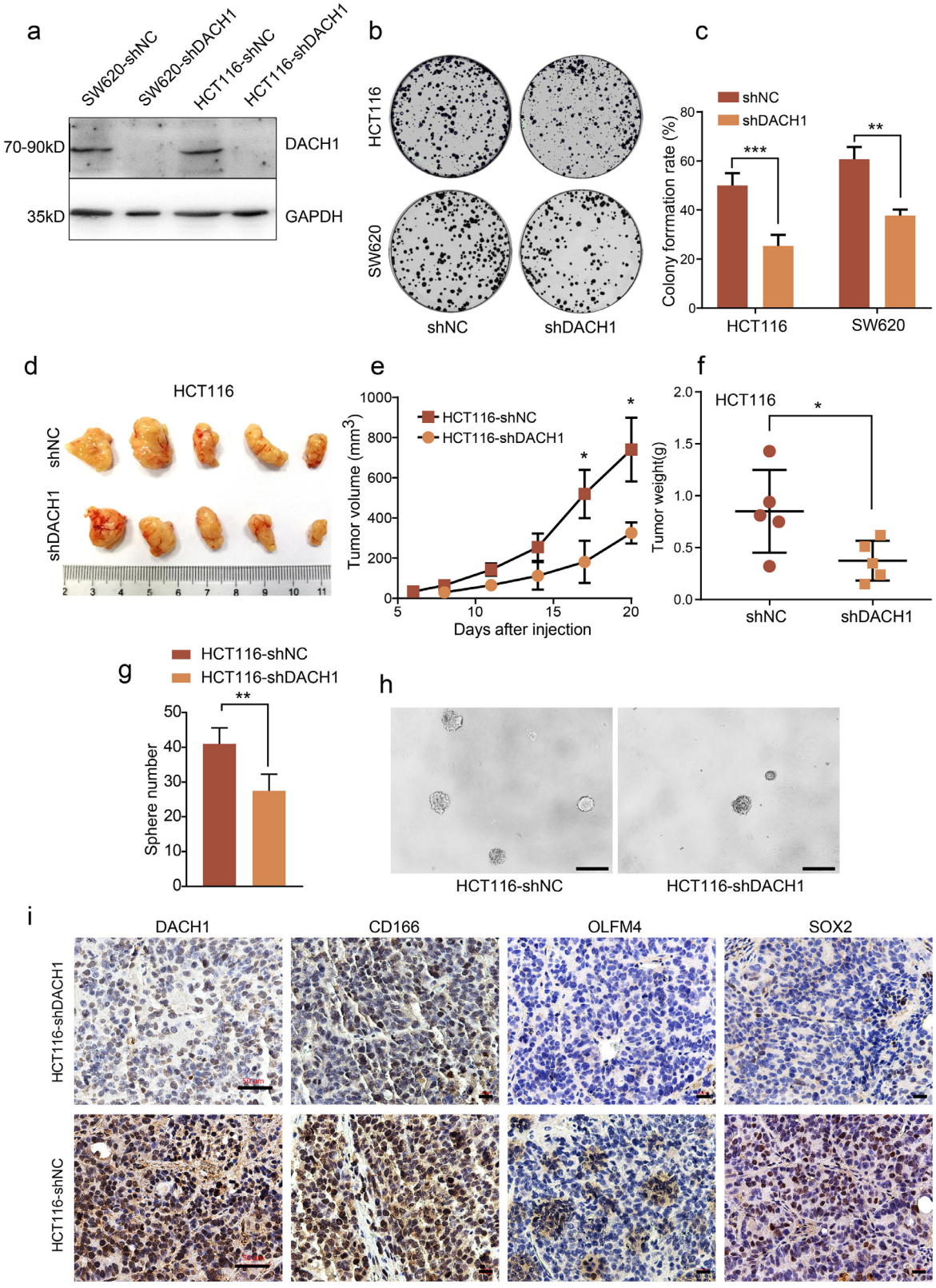

Fig. 2. DACH1 suppression inhibits colon cancer cell growth in vitro and in vivo. The efficiency of DACH1 knockdown in colon cancer cell lines was confirmed by western blotting (a). Cells with knockdown of DACH1 displayed increased inhibition of cell growth compared with control cells (b and c, experiments were performed in triplicate). Representative images of xenografts at the end of the study (d) showing decreased growth in HCT116-shDACH1 cells compared with the control, including tumour volumes (e) and tumour weights (f). Knockdown of DACH1 significantly reduced the number of spheres formed by HCT116 cells (g and h, scale bar=200 μm). IHC assays showed weaker CD166, OLFM4 and SOX2 staining in xenografts in which DACH1 was knocked down than in the controls (i). For DACH1 staining images, the scale bars=50 μm, and for CD166, OLFM4 and SOX2 staining images, the scale bars=20 μm. For 2c, 2e, 2f and 2 g, $^{*}P < 0.05$, $^{**}P < 0.01$, $^{***}P < 0.001$, Student's t-test. Error bars: mean±SD.

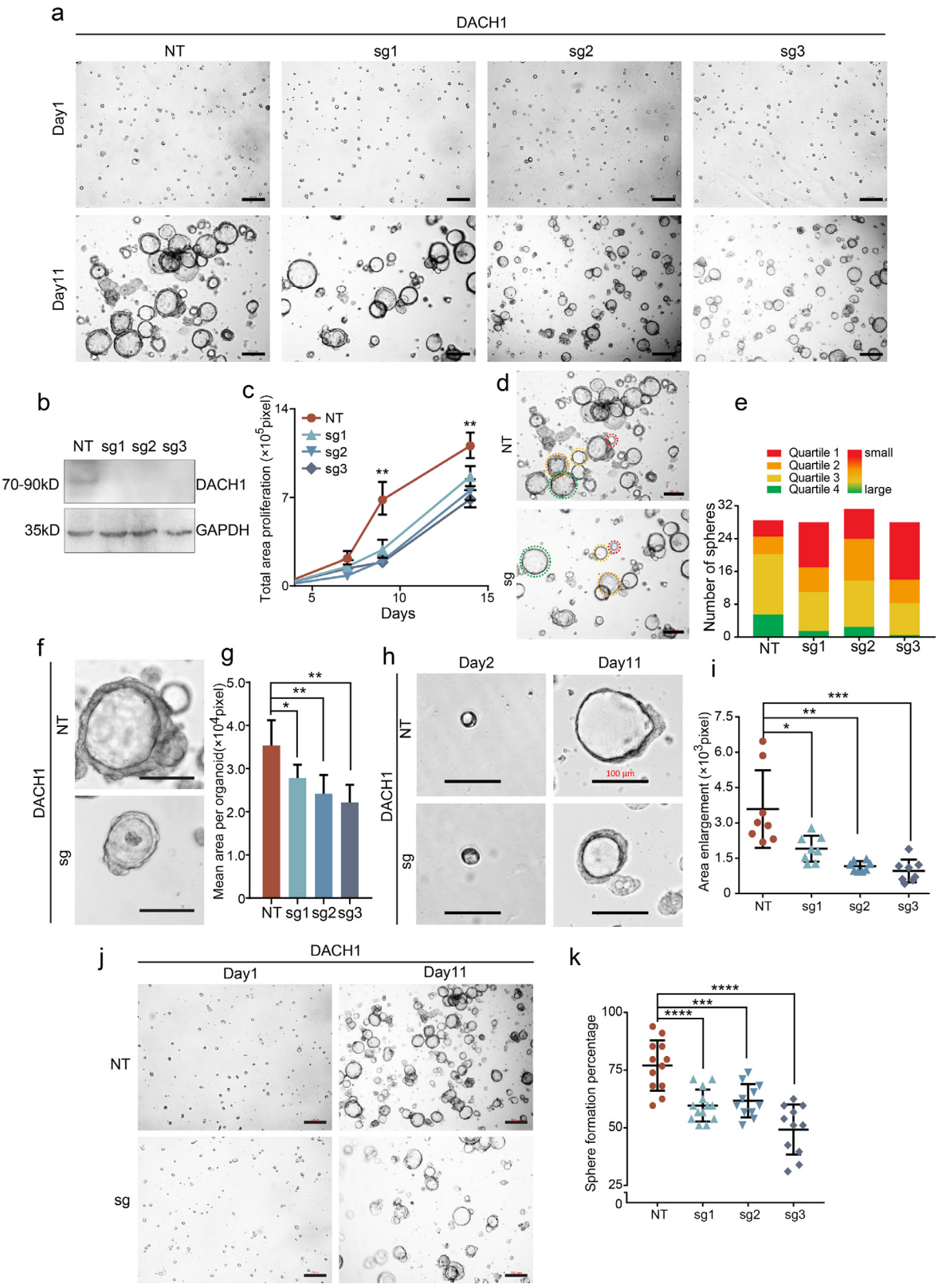

Fig. 3. DACH1 stimulated CRC organoid formation. a. Representative images of the CRC organoid spheres. Sphere areas decreased in all the DACH1-knockout organoids (transfected with 3 single guide RNAs, sgRNAs, designated as sg1, sg2 and sg3) compared with that in the NT group. The scale bars for the upper row=100 μm, and the scale bars for the lower row=200 μm. b. DACH1 was efficiently knocked out in sgRNA-transfected organoids, as detected by WB. c. Total sphere areas decreased in the DACH1 sgRNA-transfected group compared with those in the NT group. d-e. The organoid areas in the presence of DACH1 expression were within the lower quartile more than the control; scale bars =200 μm. f-g. The average sphere areas of DACH1 knockout organoids were decreased compared with those in the NT control; scale bar=100 μm. h-i. The sphere growth rates in NT organoids were higher than those in the DACH1-knockout group; scale bar=100 μm. j-k. The organoid forming efficiency was decreased by DACH1 knockout. The scale bars in the left column=100 μm, and the scale bars in the right column=200 μm. For 3c, 3 g, 3i and 3k, $^{*}P < 0.05$, $^{**}P < 0.01$, $^{***}P < 0.001$, $^{****}P < 0.0001$, Student's t-test. Error bars: mean±SD.

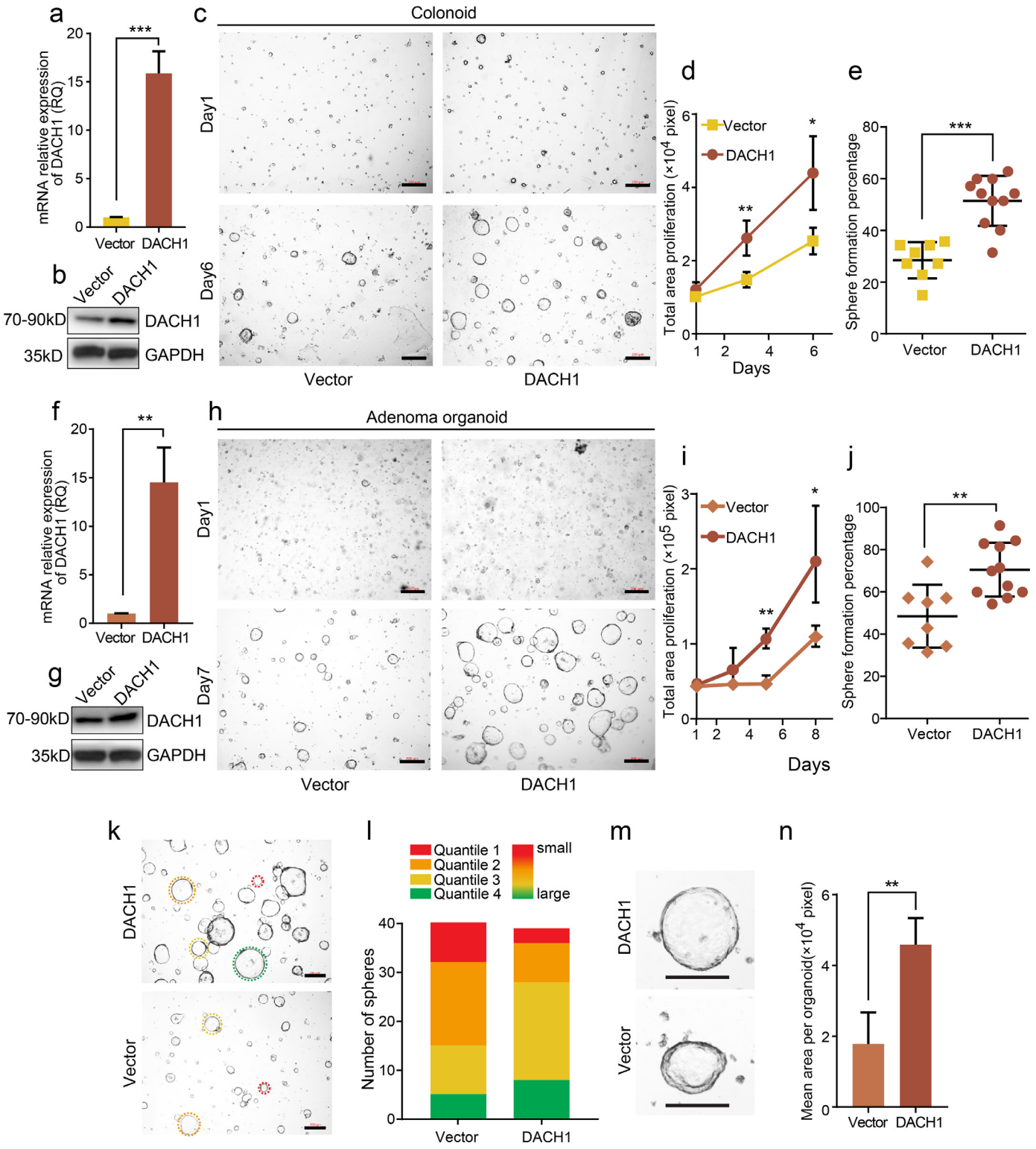

Fig. 4. DACH1 overexpression enhances the growth of organoids derived from normal colon crypts and colorectal adenomas. DACH1 overexpression efficiency was verified by qRT-PCR (experiments were performed in triplicate) (a) and western blot (b). c. Overexpression of DACH1 enhanced the sphere formation of organoids derived from normal colon crypts (colonoid) compared with the control; scale bars=200 μm d. Overexpression of DACH1 significantly enhanced colonoid proliferation compared with the vector group. e. Overexpression of DACH1 significantly enhanced the colonoid formation rate compared with the control. DACH1 overexpression was verified by qRT-PCR (experiments were performed in triplicate) and western blot (f and g). h. Adenoma organoids with DACH1 overexpression expanded to almost twice the size of the control organoids; scale bars=200 μm. i. Overexpression of DACH1 significantly enhanced the proliferation of organoids derived from colorectal adenoma compared with the control. j. The adenoma organoid formation efficiency was improved by DACH1 overexpression. k-l. The organoid areas of DACH1-overexpressing organoids were within the lower quartile more than the control; scale bars=200 μm. m-n. The average adenoma organoid areas in DACH1-overexpressing organoids were significantly larger than those in the control; scale bars=100 μm. For 4a, 4d, 4e, 4f, 4i, 4j and 4n, $^{*}P < 0.05$, $^{**}P < 0.01$, $^{***}P < 0.001$, Student's t-test. Error bars: mean±SD.

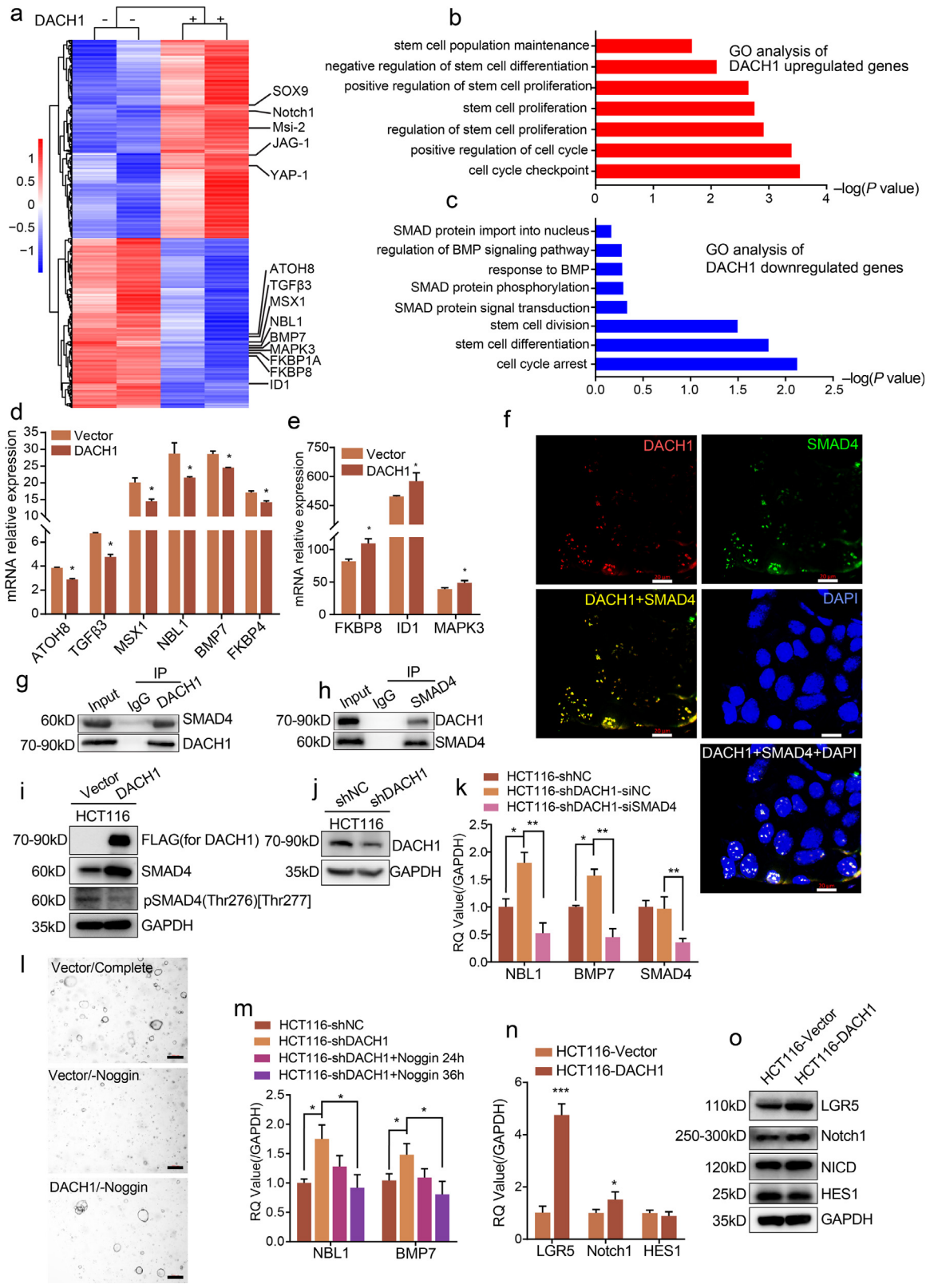

Fig. 5. DACH1 promotes adenomas organoid formation via modulating BMP signalling. a DACH1 overexpression induced upregulation of cancer stem cell marker genes. b and c. Gene Ontology (GO) analysis showed that DACH1 overexpression induced the upregulation of stem cell signature genes and the downregulation of cell cycle arrest signature genes. d and e. DACH1 induced the downregulation of ATOH8, TGFβ3, MSX1, NBL1, BMP7, and FKBP4 and the upregulation of FKBP8, ID1, and MAPK3 (experiments were performed in triplicate). f. IF images showing the colocalization of SMAD4 and DACH1 in the nuclei; scale bars=20 μm g-h. DACH1 coprecipitated endogenous SMAD4. Reverse immunoprecipitation was confirmed with an anti-SMAD4 antibody. i. DACH1 overexpression increased the protein level of SMAD4 and decreased the level of phosphorylated SMAD4 (Thr276) [Thr277]. j and k. DACH1 knockdown led to an increase of the mRNA levels of NBL1 and BMP7 compared with the shNC group, and siRNA mediated SMAD4 knockdown in HCT116-shDACH1 cells eliminated the increase. l. DACH1 overexpression was sufficient to compensate for the withdrawal of Noggin and supported the formation of adenoma organoids. m. Addition of Noggin into the culture medium for 24 and 36 h decreased the mRNA levels of NBL1 and BMP7, which were increased by DACH1 knockdown in HCT116 cells. n and o. Overexpression of DACH1 upregulates LGR5, Notch1 and the protein level of NICD, while did not induce significant upregulation of HES1. Scale bars=20 μm. For 5d, 5e, 5k, 5 m and 5n, $^{**}P < 0.01$, $^{*}P < 0.05$, Student's t-test. Error bars: mean±SD.

addition of Noggin, which is in accordance with the results of SMAD4 interference (Fig. 5k, $^{*}P < 0.05$, $^{**}P < 0.01$, Student's t-test). Hence, DACH1 was further indicated to promote cell stemness by the inhibition of the BMP signalling pathway.

To further reveal how did DACH1 promote the stemness of intestinal cells, we detected the changes DACH1 made to classical Notch pathway (Fig. 5a) and classical intestinal stem marker LGR5. We found that DACH1 upregulated Notch1 at both the mRNA level and protein level, and accordingly, the protein level of Notch intracellular domain (NICD) showed a slight increase. However, DACH1 did not induce the upregulation of HES1 (Fig. 5n and 5o, $^{*}P < 0.05$, $^{***}P < 0.001$, Student's t-test). It's been found that DACH1 is upregulated in LGR5+ ISCs, so we also detected the effect of DACH1 on LGR5. As shown in Fig. 5n ($^{*}P < 0.05$, $^{**}P < 0.01$, Student's t-test) and 5o, overexpression of DACH1 boosted the expression of LGR5 in HCT116 cells. These results indicate that DACH1 promoted intestinal cell stemness by enhancing classical stem cell pathways.

Similar as Noggin, EGF and R-spondin were excluded from the medium. However, DACH1 overexpression did not reverse the organoid formation inhibition caused by the absence of EGF or R-spondin (Supplementary data, Fig. S2). Thus, DACH1 does not affect the efficiency of organoid formation mediated by EGF or R-spondin.

4. Discussion

Despite the controversy about the role of DACH1 in CRC [10–13], in this study, we identified DACH1 as a potential indicator of intestinal stem cells and cancer stem cells in mouse small and large intestine as well as human CRC. In the small and large intestine, DACH1 expression was observed in the morphologically distinct undifferentiated cells in the crypt base. This distribution of DACH1 expression closely resembles that of markers for intestinal stem cells [3]. In this study, we cultured organoids derived from the normal colon crypt, colorectal adenoma and CRC and determined that DACH1 supported the proliferation and undifferentiated state of stem cells in vitro, indicating that DACH1 plays a role in promoting cell stemness in normal crypt base cells, colorectal adenoma and CRC. How DACH1 promotes CRC tumorigenesis was obscure [13], and now we provide evidence that DACH1 plays an essential role in inducing stem cell self-renewal and tumorigenesis through direct upregulation of stem cell signature genes, which it accomplishes by binding to SMAD4 and repressing the BMP signalling pathway. Hence, DACH1 expression is a marker of intestinal stem cells and contributes to colorectal tumorigenesis.

Restricted crypt base expression of DACH1 protein in human and mouse intestines was illustrated in our study. DACH1 exhibited a similar distribution pattern to that of LGR5 and OLFM4, which are suggested markers of stem cells in humans [3,19]. In addition to stem cells, Paneth cells, which support the stem cell niche, also account for a proportion of cells at the crypt base. However, our data did not conclusively demonstrate an overlap between DACH1-overexpressing cells and Paneth cells, indicating that DACH1 is expressed exclusively in colon crypt stem cells. In our study, we found that overexpression of DACH1 could upregulate the mRNA and protein of LGR5. This might explain the distribution pattern and the location of DACH1, besides, this finding also provided an explanation for why DACH1 is highly expressed in LGR5+ intestinal stem cells and colorectal tumours.

DACH1 was consistently expressed in human CRC. In the survival analysis, high DACH1 expression was markedly associated with worse prognosis, indicating that DACH1 may serve as a potential prognostic marker of poor prognosis in CRC. However, some studies in non-intestinal cell types have identified an antiproliferative role for DACH1 [7,20], suggesting that DACH1 may play different roles depending on the cell type and/or context. Interestingly, a recent research found out that DACH1 was expressed less in male breast cancer than in female breast cancer [21]. In our study, the percentage of female patients that express high level of DACH1 was found to be higher than male patients even the statistical significance is not reached (Table 1). This accordance expression pattern of DACH1 hints that in different cancers, the expression of DACH1 might be correlated to sex and/or hormone.

Our organoids were cultured in systems developed by Sato et al. [14]. Consistent with a previous report [22], the formation efficiency of colonoids was approximately 30%, and DACH1 overexpression increased the efficiency to approximately 60%. Moreover, DACH1-overexpressing colonoids developed significantly earlier than the control colonoids, suggesting that DACH1 has a function that is similar to the function previously reported for Sox9 by Ramalingam et al. [23]. Furthermore, DACH1 significantly enhanced the growth and sphere formation efficiency of adenoma organoids. To explore the factors associated with DACH1, we performed RNA-seq analysis and revealed an association between DACH1 and the BMP signalling pathway. Accordingly, aberrant BMP signalling leads to intestinal polyp growth and CRC development [24]. SMAD4, as the Co-SMAD of the BMP signalling pathway, may allow R-SMADs (SMAD1, 5 and 8) to bind, form complexes, translocate into the nucleus and modulate target genes when BMPRI is phosphorylated and activated [16,25,26]. Therefore, SMAD4 is a pivotal regulator in the BMP signalling pathway for maintaining intestinal epithelial homoeostasis and inhibiting stem cell activity [27]. CoIP and reciprocal CoIP demonstrated an interaction between DACH1 and SMAD4. Inhibition of stemness in LGR5+ stem cells may occur through SMAD-associated transcriptional repression of stem cell signature genes, and this inhibitory effect is independent of Wnt/β-catenin signalling [5]. Therefore, we depleted key factors (Noggin, EGF and R-spondin) in the colorectal organoid culture medium [14,15,28]. Adenoma organoid formation decreased without Noggin, but DACH1 overexpression compensated for the effect of Noggin depletion. Besides, we also found that in HCT116 cells, both addition of Noggin and interference of SAMD4 reduced the boosted expression of NBL1 and BMP7 by DACH1 knockdown, thus further confirming that the role of DACH1 is tightly associated with the BMP signalling pathway. Here, we displayed evidence for an essential role of DACH1 in maintaining organoid self-renewal through direct binding of SMAD4 and release of stem cell signature genes. DACH1 could enhance the hyperproliferation of the intestinal epithelium by inducing stem cell expansion.

In conclusion, we demonstrated an essential role of DACH1 in maintaining intestinal stem cell self-renewal and colorectal tumour development, which it accomplishes by interacting with SMAD4 and inhibiting the BMP signalling pathway. Moreover, we propose DACH1 as a marker of intestinal stem cells and as an independent marker for colorectal cancer prognosis. Additionally, our findings may facilitate further studies of intestinal stem cell biology and colorectal tumorigenesis.

Declarations of Competing Interest

All authors declare that they have no conflicts of interest.

Funding sources

This work was supported by National Natural Science Foundation of China (Grants No. 31470826 (to Hua), 31670858 (to Hua), and 81672374(to Cai)), Science and Technology Commission of Shanghai Municipality (Grant No.18401933400 (to Peng)), National Natural Science Foundation of China (Grant No. 81972244 (to Hu)), Shanghai Anticancer Association EYAS PROJECT (SACA-CY1A05 (to Li)), and Fudan University Shanghai Cancer centre Basic and Clinical Translational Research Seed Foundation (Grant No. YJZZ201802 (to Cai)).

The funders had no role in the study design, data collection, data analysis, data interpretation and writing of the report.

Authors' contributions

XH designed the study, performed most of the experiments, analysed the data and cowrote the manuscript. LZ organized the results, analysed the data, participated in some experiments, cowrote the manuscript and organized the figures. YL participated in the design of the study, participated in some experiments and analysed the data. WD, XM, XG, XR, GF, RW, MP, QG, and XX participated in some experiments and/or data analysis. XX, YZ, JG and ZZ provided support for this study. JG and ZZ provided suggestions. SC, JP and GH conceptualized, designed and directed the project and cowrote the manuscript. All authors read and approved the manuscript.

Supplementary materials

Supplementary material associated with this article can be found in the online version at doi:10.1016/j.ebiom.2020.102800.

References

[1] Sato T, Vries RG, Snippert HJ, van de Wetering M, Barker N, Stange DE, et al. Single Lgr5 stem cells build crypt-villus structures in vitro without a mesenchymal niche. Nature 2009;459(7244):262–5.
[2] Vermeulen L, Snippert HJ. Stem cell dynamics in homeostasis and cancer of the intestine. Nature Rev Cancer 2014;14(7):468–80.
[3] Barker N, van Es JH, Kuipers J, Kujala P, van den Born M, Cozijnsen M, et al. Identification of stem cells in small intestine and colon by marker gene Lgr5. Nature 2007;449(7165):1003–7.
[4] Barker N, Ridgway RA, van Es JH, van de Wetering M, Begthel H, van den Born M, et al. Crypt stem cells as the cells-of-origin of intestinal cancer. Nature 2009;457(7229):608–11.
[5] Qi Z, Li Y, Zhao B, Xu C, Liu Y, Li H, et al. BMP restricts stemness of intestinal Lgr5(+) stem cells by directly suppressing their signature genes. Nat Commun 2017;8:13824.
[6] Liu Q, Li A, Yu S, Qin S, Han N, Pestell RG, et al. DACH1 antagonizes CXCL8 to repress tumorigenesis of lung adenocarcinoma and improve prognosis. J Hematol Oncol 2018;11(1):53.
[7] Cui Q, Kong D, Li Z, Ahiable P, Wang K, Wu K, et al. Dachshund 1 is Differentially Expressed Between Male and Female Breast Cancer: a Matched Case-Control Study of Clinical Characteristics and Prognosis. Clin Breast Cancer 2018.
[8] Cheng Q, Ning D, Chen J, Li X, Chen XP, Jiang L. SIX1 and DACH1 influence the proliferation and apoptosis of hepatocellular carcinoma through regulating p53. Cancer Biol Ther 2018;19(5):381–90.
[9] Bu XN, Qiu C, Wang C, Jiang Z. Inhibition of DACH1 activity by short hairpin RNA represses cell proliferation and tumor invasion in pancreatic cancer. Oncol Rep 2016;36(2):745–54.
[10] Cao J, Yan XR, Liu T, Han XB, Yu JJ, Liu SH, et al. MicroRNA-552 promotes tumor cell proliferation and migration by directly targeting DACH1 via the Wnt/beta-catenin signaling pathway in colorectal cancer. Oncol Lett 2017;14(3):3795–802.
[11] Wang P. Suppression of DACH1 promotes migration and invasion of colorectal cancer via activating TGF-beta-mediated epithelial-mesenchymal transition. Biochem Biophys Res Commun 2015;460(2):314–9.
[12] Yan W, Wu K, Herman JG, Brock MV, Fuks F, Yang L, et al. Epigenetic regulation of DACH1, a novel Wnt signaling component in colorectal cancer. Epigenetics 2013;8(12):1373–83.
[13] Vonlanthen J, Okoniewski MJ, Menigatti M, Cattaneo E, Pellegrini-Ochsner D, Haider R, et al. A comprehensive look at transcription factor gene expression changes in colorectal adenomas. BMC Cancer 2014;14:46.
[14] Sato T, Stange DE, Ferrante M, Vries RG, Van Es JH, Van den Brink S, et al. Long-term expansion of epithelial organoids from human colon, adenoma, adenocarcinoma, and Barrett's epithelium. Gastroenterology 2011;141(5):1762–72.
[15] Sato T, van Es JH, Snippert HJ, Stange DE, Vries RG, van den Born M, et al. Paneth cells constitute the niche for Lgr5 stem cells in intestinal crypts. Nature 2011;469(7330):415–8.
[16] Miyazono K, Maeda S, Imamura T. BMP receptor signaling: transcriptional targets, regulation of signals, and signaling cross-talk. Cytokine Growth Factor Rev 2005;16(3):251–63.
[17] Massague J. TGFbeta signalling in context. Nat Rev Mol Cell Biol 2012;13(10):616–30.
[18] He XC, Zhang J, Tong WG, Tawfik O, Ross J, Scoville DH, et al. BMP signaling inhibits intestinal stem cell self-renewal through suppression of Wnt-beta-catenin signaling. Nat Genet 2004;36(10):1117–21.
[19] van der Flier LG, Haegebarth A, Stange DE, van de Wetering M, Clevers H. OLFM4 is a robust marker for stem cells in human intestine and marks a subset of colorectal cancer cells. Gastroenterology 2009;137(1):15–7.
[20] Chen K, Wu K, Cai S, Zhang W, Zhou J, Wang J, et al. Dachshund binds p53 to block the growth of lung adenocarcinoma cells. Cancer Res 2013;73(11):3262–74.
[21] Cui Q, Kong D, Li Z, Ahiable P, Wang K, Wu K, et al. Dachshund 1 is differentially expressed between male and female breast cancer: a matched case-control study of clinical characteristics and prognosis. Clin Breast Cancer 2018;18(5):e875–e82.
[22] Ahmad AA, Wang Y, Gracz AD, Sims CE, Magness ST, Allbritton NL. Optimization of 3-D organotypic primary colonic cultures for organ-on-chip applications. J Biol Eng 2014;8:9.
[23] Ramalingam S, Daughtridge GW, Johnston MJ, Gracz AD, Magness ST. Distinct levels of Sox9 expression mark colon epithelial stem cells that form colonoids in culture. Am J Physiol Gastrointestinal Liver Physiol 2012;302(1):G10–20.
[24] Kim BG, Li C, Qiao W, Mamura M, Kasprzak B, Anver M, et al. Smad4 signalling in T cells is required for suppression of gastrointestinal cancer. Nature 2006;441(7096):1015–9.
[25] Feng XH, Derynck R. Specificity and versatility in tgf-beta signaling through Smads. Annu Rev Cell Dev Biol 2005;21:659–93.
[26] Moustakas A, Heldin CH. The regulation of TGFbeta signal transduction. Development 2009;136(22):3699–714.
[27] Reynolds A, Wharton N, Parris A, Mitchell E, Sobolewski A, Kam C, et al. Canonical Wnt signals combined with suppressed TGFbeta/BMP pathways promote renewal of the native human colonic epithelium. Gut 2014;63(4):610–21.
[28] Miyoshi H, Ajima R, Luo CT, Yamaguchi TP, Stappenbeck TS. Wnt5a potentiates TGF-beta signaling to promote colonic crypt regeneration after tissue injury. Science 2012;338(6103):108–13.